Journal of ELECTRONIC MATERIALS, Vol. 42, No. 12, 2013
DOI: 10.1007/s11664-013-2747-0
© 2013 TMS

Low-Temperature Processing of PZT Thick Film by Seeding and High-Energy Ball Milling and Studies on Electrical Properties

SOMA DUTTA,[1,2] A. ANTONY JEYASEELAN,[1] and S. SRUTHI[1]

1.—Materials Science Division, National Aerospace Laboratories, Council of Scientific and Industrial Research, Bangalore 560017, India. 2.—e-mail: som@nal.res.in

Lead zirconate titanate thick film with molecular formula $PbZr_{0.52}Ti_{0.42}O_3$ (PZT) was prepared by a modified conventional sol–gel method through seeding and high-energy ball milling, resulting in perovskite phase formation at lower temperatures. The ball-milling time was optimized by keeping the seed particle loading (5 wt.%) constant in the sol–gel solution. This methodology helped in reduction of the crystalline phase formation temperature to 300°C, which is much lower than that reported in the literature (450°C). The well-established perovskite phase was confirmed by x-ray diffraction (XRD) analysis. Scanning electron microscopy (SEM) of PZT films revealed uniform and crystalline microstructure. Film prepared by this methodology showed higher spontaneous polarization (2.22 μC/cm^2), higher capacitance (1.17 nF), and low leakage current density (18 μA/cm^2). The results obtained from ferroelectric characterization showed a strong correlation with the XRD and SEM results.

Key words: PZT thick film, seeding, high-energy ball milling, XRD, ferroelectric

INTRODUCTION

Lead zirconate titanate material has been extensively investigated by researchers for its good piezoelectric, ferroelectric, and optical properties.[1–4] In the late 1980s, use of bulk $PbZr_{0.52}Ti_{0.42}O_3$ (PZT) was increasingly supplemented by thin/thick films due to their integration into semiconductor chips with the advent of nonvolatile random-access memory (NVRAM) devices. PZT materials in thick film (10 μm to 20 μm) form have been used in high-frequency transducers and vibration control devices for their actuation properties.[5] Fabrication of thicker (i.e., 100 μm to 500 μm) films using methods like tape casting and screen printing suffers from drawbacks due to nonuniformity, the requirement for a high sintering temperature ($\sim$1200°C) for film densification, and the lack of reproducibility in their properties.[6,7] It is a very challenging task to fabricate thicker films at low temperature. Though the sol–gel-based chemical method has been widely used for fabrication of such films, it is not suitable for production of thick films higher than 3 μm due to the requirement of large deposition cycles. The present research aims at obtaining thicker (up to 100 μm) films at lower processing temperatures ($<$400°C) to aid their smooth integration into semiconductor device compounds.[8]

Many methodologies have been tried for low-sintering phase formation by the aerosol deposition method,[9,10] laser annealing processes,[11] microwave irradiation using a magnetic field,[12] PZT ink,[13] etc. The effect of seeding on reduction of firing temperature (450°C to 650°C) for fabrication of PZT thick films has been reported earlier.[14–16] A novel approach to reduce the processing temperature of PZT thick films below 450°C using the combined effect of high-energy ball milling and seeding (i.e., a small percentage of crystalline PZT seeds) on the

(Received February 11, 2013; accepted August 16, 2013; published online September 19, 2013)

PZT precursor solution has been attempted. The present methodology of low-temperature PZT thick-film preparation can address all the drawbacks related to high-temperature sintering. This paper presents preparation, microstructural characterisation, and studies on ferroelectric properties of the films to verify the quality of the material for device fabrication.

EXPERIMENTAL PROCEDURES

Preparation

Thick film of PZT on aluminum substrate was grown by a modified sol–gel method using processed PZT powder as seed to reduce the crystallization temperature. Powder was prepared for seeding by the sol–gel method as reported elsewhere.[17] The processed powder was ball-milled for 1 h to achieve submicron particle size, then added to PZT sol solution to 5 wt.%.[18] Sol was prepared by dissolving lead acetate trihydrate in glacial acetic acid. Zirconium *n*-propoxide and titanium(IV) isopropoxide were taken in *n*-propanol as per the stoichiometry and added to the lead precursor solution under constant stirring. After adding PZT seed to the sol, ethylene glycol was added to the stock solution and ball-milled for 15 h, 30 h, and 40 h using a FRITSCH Pulverisette 6 at room temperature. The prepared composite sol (15-h-, 30-h-, or 40-h-milled) was deposited on aluminum substrate by spin-coating at 8000 rpm for 50 s and dried (pyrolized) at 300°C for 10 min on a preheated hot plate in open atmosphere. The films were annealed at 300°C (heating rate 10°C/min) for 1 h in a furnace under oxygen-rich atmosphere.

Characterization

The polycrystalline phase formation of PZT thick film was investigated by x-ray diffraction analysis, and the surface morphology was observed by scanning electron microscopy (SEM). The compositional study of the PZT films was carried out by energy-dispersive x-ray (EDX). For electrical characterization, an aluminum top electrode of size 2 mm^2 was deposited by vacuum deposition technique using a metal mask. Ferroelectric properties were measured using a thin-film analyzer (aixACT 2000).

RESULTS AND DISCUSSION

X-Ray Diffraction (XRD) Analysis

Figure 1a–c shows XRD patterns of annealed PZT thick (5 μm) films prepared by milling sol solutions for 15 h, 30 h, and 40 h. The effect of milling on the crystalline phase formation is clearly observed in the XRD patterns. In Fig. 1a, it is seen that the perovskite phase was not formed for the PZT film prepared with 15-h-milled sol. Only a few diffraction peaks were observed, which do not correspond to the perovskite phase. Figure 1b depicts the formation of

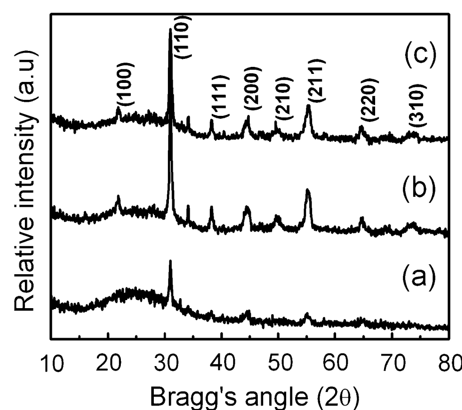

Fig. 1. XRD patterns of PZT film prepared by ball milling of composite sol for different milling times: (a) 15 h, (b) 30 h, and (c) 40 h.

the perovskite phase when the milling time was increased to 30 h. Clear and well-established perovskite peaks of the seeded PZT film were seen at $2\theta = 22.5°$ (100), 32° (110), 34° (101), 38° (111), 44.2° (200), and 55° (211), as reported elsewhere.[16] The presence of tetragonal splitting at 44° (200) and 55° (211) provides evidence of perovskite phase formation. With increase in ball-milling time from 30 h to 40 h, the peak intensity was reduced, indicating further decrease in grain size and disintegration of crystal phases. The tetragonal splitting found in the 30-h-ball-milled sample was converted to a doublet ($2\theta = 44°$) and singlet ($2\theta = 55°$) with 40 h of milling (Fig. 1c). The XRD results confirm that the combined effect of seeding and high-energy ball milling on the sol–gel solution resulted in decreasing the phase formation temperature to 300°C. Experiments on milling of sol–gel solution without seeding, as well as seeding without milling, were attempted to investigate their effects on lowering the temperature, but these procedures did not reduce the phase formation temperature below 450°C.

SEM Analysis

Figure 2a–c shows the surface morphology of PZT films of thickness 5 μm, prepared from the composite solution (PZT sol + seed) after different durations of ball milling (15 h, 30 h, and 40 h) and annealing at 300°C for 1 h. The microstructure of the PZT film prepared from the composite solution after 15 h milling showed partially grown crystalline grains. It was observed from the microstructure that grain growth was not complete after 15 h of milling to form the crystalline single phase of PZT perovskite. The submicron-size spherical grains seen in Fig. 2a are attributed to the crystalline PZT seeds used in the sol. The microstructure in Fig. 2a also shows cracks and voids that may be due to elimination of organic additives from the sol–gel precursor during annealing. When the milling time was increased to 30 h, the microstructure appeared

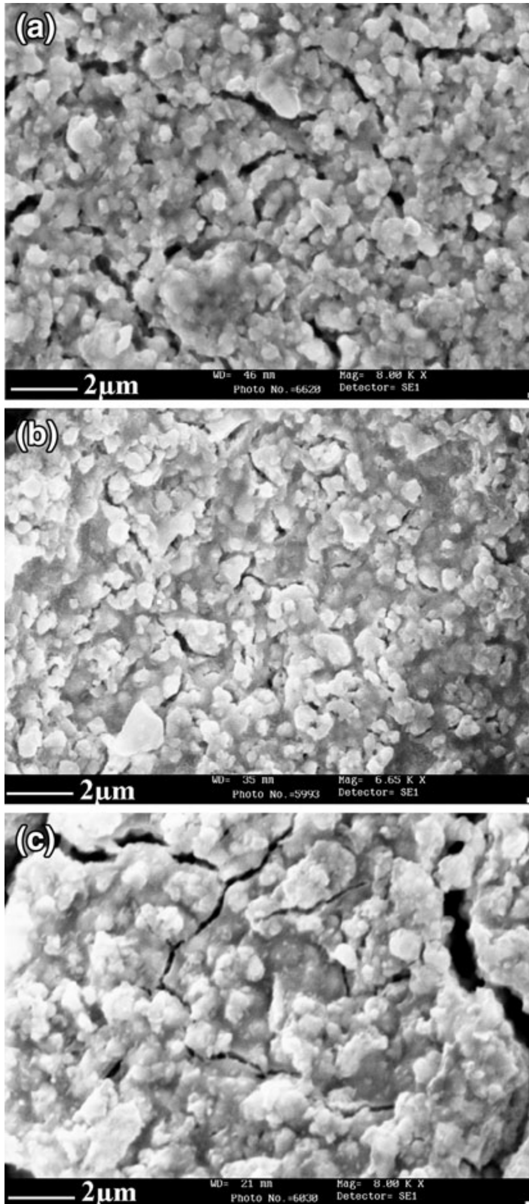

Fig. 2. Scanning electron micrographs of PZT films prepared by ball milling of composite sol for different durations: (a) 15 h, (b) 30 h, and (c) 40 h.

more uniform with distributed spherical grains (Fig. 2b) and was free from voids and cracks. Milling of the composite sol for 30 h facilitated formation of crystalline PZT phase at 300°C. The advanced grain growth due to annealing of the film helped to fill the voids and cracks. In the 40-h-milled sample, the microstructure was nonuniform (Fig. 2c) because of the disintegration of larger grains into nanoscale particles which became agglomerated during annealing, introducing larger cracks into the structure.

The energy-dispersive x-ray (EDX) study (Fig. 3) confirmed the stoichiometric composition of PZT

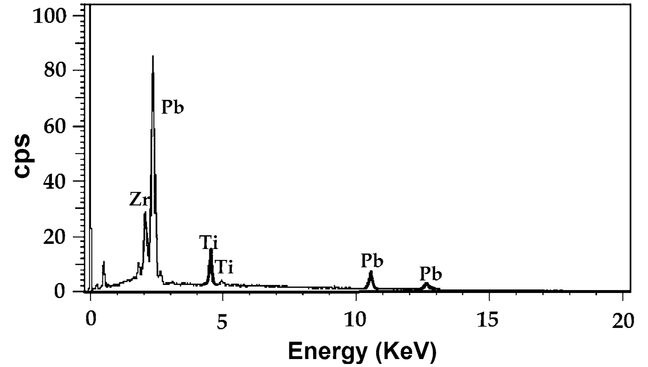

Fig. 3. Energy-dispersive x-ray plot for $PbZr_{0.52}Ti_{0.48}O_3$.

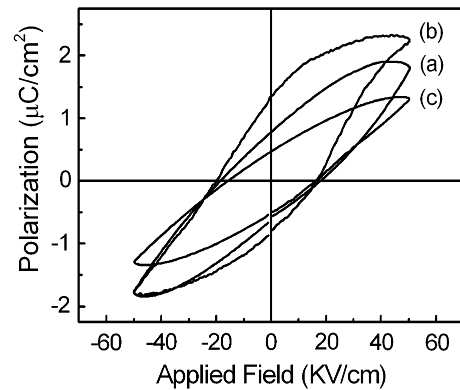

Fig. 4. *P–E* hysteresis curves of PZT films prepared by ball milling of composite sol for different milling durations: (a) 15 h, (b) 30 h, and (c) 40 h.

film with Pb/(Zr + Ti) ratio of 1.0161 and Zr/Ti ratio of about 52/48.

Electrical Characterization

P–E Characterization

Figure 4 shows a typical plot of polarization versus electric field (*P–E* hysteresis loop) of PZT film (thickness ~5 μm) deposited from the composite sol after milling for several hours and annealing at 300°C. All the films prepared from the 15-h-, 30-h-, and 40-h-milled samples exhibited a ferroelectric hysteresis loop. As observed from this figure, the 30-h-milled sample showed improved remanent (1.27 $\mu C/cm^2$) and spontaneous polarization (2.22 $\mu C/cm^2$), comparable to values reported in the literature.[19] The low polarization values of the 15-h- and 40-h-milled samples correlate well with the microstructure data (Fig. 2a, c). *P–E* loop saturation was seen only for the 30-h-milled sample (Fig. 4b) but was not observed for the 15-h- (Fig. 4a) and 40-h-milled samples (Fig. 4c). It can be inferred that this enhancement in polarization (for 30 h milling) is due to the uniform microstructure of the close-packed grains, which facilitated the dipole moment through domain-wall movement.

The low polarization value for the 15-h-milled sample is inferred to be due to the nonuniform growth and distribution of polycrystalline grains because of insufficient milling time leading to lower milling energy. Milling for reduced duration did not completely convert the amorphous sol into the crystalline phase. This hinders domain switching and the dipole moment, thereby reducing the polarization. However, the presence of crystalline PZT (used as seed) to some extent aids in increasing the dipole moment. The second parameter affecting the polarization is the lower density of the film.

In the case of 40-h milling, the lowest polarization was observed; this is due to the reduction in the grain size from submicron to nanoscale induced by the excessive milling time. Since nanograins prevent easy movement of dipole domains, this leads to lower remanent polarization.[2] However, the *P–E* hysteresis loop results confirm the formation of a crystalline single phase of PZT at lower temperatures. The inflated shape of the *P–E* loop at high electric field is due to the increase in charge leakage occurring through the voids because of the poor density of the film.

C–V Characterization

Figure 5 shows capacitance versus voltage (*C–V*) plots of the PZT films prepared by using the composite sol milled for different durations. The dependence of the capacitance on the voltage shows a strong butterfly loop which confirms the presence of ferroelectricity in these materials. In Fig. 5b, it is observed that the 30-h-milled composite sample shows a higher capacitance value of 1.17 nF around 6 V. The capacitance values obtained for the 15-h- (0.62 nF) and 40-h-milled (0.92 nF) samples are comparable to reported results.[20] The homogeneous dispersion of the PZT crystals makes the capacitance value higher for the 30-h-milled sample, as seen in the case of the *P–E* curves. For the 15-h-milled sample, the noncrystalline sol–gel additives, voids and cracks, facilitated easy conduction paths causing discharge that decreases the capacitance value at higher voltages. In the case of the 40-h-milled sample, the moderate capacitance value as compared with the 15-h-milled sample was due to a lower discharge because of less voids and cracks (improved density), which does not aid easy passage of charge conduction.

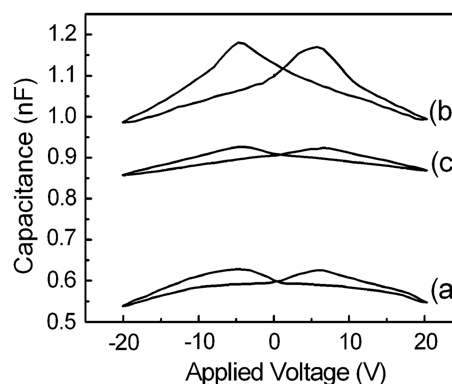

Fig. 5. *C–V* plots for PZT films prepared by ball milling of composite sol for different milling durations: (a) 15 h, (b) 30 h, and (c) 40 h.

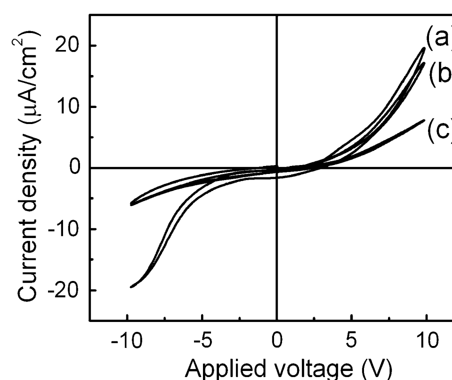

Fig. 6. Variation of leakage current density of PZT films prepared by ball milling of composite sol for different milling durations: (a) 15 h, (b) 30 h, and (c) 40 h.

I–V Characterization

In addition to *C–V* characterization, leakage current density versus applied voltage (*I–V*) characteristics of the composite films were also measured. This is one of the important properties to study to ensure the reliability of a material for usage in capacitors. Figure 6 shows leakage current characteristic plots of the composite films prepared from 15-h-, 30-h-, and 40-h-milled sol solutions. The plot of leakage current (μA/cm^2) versus applied voltage (V) helps to identify the transition of the material's conduction from ohmic (tunneling of electrons) to Schottky (thermionic emission of electrons) at higher field. It is observed from Fig. 6a that the leakage current density of the 15-h-ball-milled PZT film indicates near-ohmic behavior up to applied voltage of 3 V. There was a change in the slope of the *I–V* curve, showing a higher current density value of 20 μA/cm^2, at 10 V. Similar results have been reported for PZT thin films at $\pm$4 V.[21] PZT films prepared by this low-temperature annealing method have density around 75% of bulk PZT. This might cause greater leakage at higher voltages, as reflected by the inflated shape of the *P–E* hysteresis loops. Films with larger grain sizes will have shorter conduction paths along grain boundaries, which causes an increase in the leakage current. It has been reported in the literature that microstructural factors such as crystal orientation and grain boundaries can also cause leakage.[22,23]

For the film made with 30-h-milled sol, it was seen that the leakage current density decreased to 18 μA/cm^2 at 10 V (Fig. 6b). This was expected due to the homogeneous, void-free structure of the crystalline PZT with submicron particle size. These are the qualities that a good film should have for use

in capacitors. The leakage current density was observed to be minimum for the 40-h-milled sample (5 μA/cm^2 to 7 μA/cm^2), which is due to the presence of nanocrystalline grains aiding intergrain depletion of grain-boundary-limited conduction.[24,25]

CONCLUSIONS

PZT thick films were prepared at 300°C by high-energy ball milling of sol–gel solution containing crystalline PZT as seed particles. The effect of seeding and ball milling was studied to optimize the phase formation temperature of 5-μm-thick PZT films. The XRD results confirmed the formation of PZT perovskite phase at low temperature for the film prepared with 30 h of milling. SEM imaging also revealed single-phase formation for the 30-h-milled sample, being void free and exhibiting uniform microstructure compared with thin films obtained from 15-h- and 40-h-milled composite sols. *P–E* hysteresis loops, *C–V* and *I–V* characteristics, were studied to verify the ferroelectric property and the reliability of the material for device applications. Structure–property correlation was established. This research provides a simple solution to the problems associated with high-temperature sintering of PZT thick films.

REFERENCES

1. H. Kueppers, T. Leueres, U. Schnakenberg, W. Mokwa, M. Hoffmann, T. Schneller, U. Boettger, and R. Waser, *Sens. Actuators A* 97, 680 (2002).
2. Z. Wang, J. Miao, and W. Zhu, *J. Eur. Ceram. Soc.* 27, 3759 (2007).
3. D.L. Corker, Q. Zhang, R.W. Whatmore, and C. Perrin, *J. Eur. Ceram. Soc.* 22, 383 (2002).
4. S.K. Pandey, A.R. James, R. Raman, S.N. Chatterjee, A. Goyal, C. Prakash, and T.C. Goel, *Phys. B* 369, 135 (2005).
5. F. Tyholdt, R.A. Dorey, R. Bredesen, and H. Raeder, *J. Electroceram.* 19, 315 (2007).
6. G. Jian, H. Qingxian, L. Sheng, D. Zhou, and F. Qiuyun, *Proc. Appl. Ceram.* 6, 215 (2012).
7. M. Dietze and M. Es-Souni, *Sens. Actuators A.* 143, 329 (2008).
8. Y.-H. Chu, C.-W. Liang, S.-J. Lin, K.-S. Liu, and I.-N. Lin, *Jpn. J. Appl. Phys.* 43, 5409 (2004).
9. M. Lebedev, J. Akedo, and Y. Akiyama, *Jpn. J. Appl. Phys.* 39, 5600 (2000).
10. J. Akedo and M. Lebedev, *Jpn. J. Appl. Phys.* 40, 5528 (2001).
11. C.-C. Chou, S.-D. Tsai, W.-H. Tu, Y.-E. Yeh-Liu, and H.-L. Tsai, *J. Sol-Gel Sci. Technol.* 42, 315 (2007).
12. Z.J. Wang, Z.P. Cao, Y. Otsuka, N. Yoshikawa, H. Kokawa, and S. Taniguchi, *Appl. Phys. Lett.* 92, 222905 (2008).
13. M. Ferrari, V. Ferrari, M. Guizzetti, and D. Marioli, *Sensors and Microsystems: AISEM 2009 Proceedings*. Lecture Notes in Electrical Engineering, Vol. 54. doi:10.1007/978-90-481-3606-3_12.
14. D.A. Barrow, T.E. Petroff, and M. Sayer, *Surf. Coat. Technol.* 76, 113 (1995).
15. D.A. Barrow, T.E. Petroff, R.P. Tandon, and M. Sayer, *J. Appl. Phys.* 81, 876 (1997).
16. Y.Z. Chen., J. Ma, L.B. Kong, and R.F. Zhang. *Mater. Chem. Phys.* 75, 225 (2005).
17. X.G. Tang, A.L. Ding, Y. Ye, and W.X. Chen, *Thin Solid Films* 423, 13 (2003).
18. A. Bardaine, P. Boy, P. Belleville, O. Acher, and F. Levassort, *J. Eur. Ceram. Soc.* 28, 1649 (2008).
19. X.N. Jiang, C. Sun, X. Zhang, B. Xu, and Y.H. Ye, *Sens. Actuators A* 87, 72 (2000).
20. B.G. Chae, Y.S. Yang, S.H. Lee, M.S. Jang, S.J. Lee, S.H. Kim, W.S. Baek, and S.C. Kwon, *Thin Solid Films* 410, 107 (2002).
21. Q.L. Zhao, M.S. Cao, J. Yuan, R. Lu, D.W. Wang, and D.Q. Zhang, *Mater. Lett.* 64, 632 (2010).
22. L.N. Gao, S.N. Song, J.W. Zhai, X. Yao, and Z.K. Xu, *J. Cryst. Growth* 310, 1245 (2008).
23. L. Zhou, X.-F. Wang, Q. Han, J.-C. Wu, and Z.-Y. Li, *Appl. Phys. Lett.* 96, 063301 (2010).
24. S.H. Hu, G.J. Hu, X.J. Meng, G.S. Wang, J.L. Sun, S.L. Guo, J.H. Chu, and N. Dai, *J. Cryst. Growth* 260, 109 (2004).
25. B.A. Boukamp, M.T.N. Pham, D.H.A. Blan, and H.J.M. Bouwmeester, *Solid State Ionics* 170, 239 (2004).